Earthquakes and Structures, *Vol. 4, No. 5 (2013) 489-508*
DOI: http://dx.doi.org/10.12989/eas.2013.4.5.489

Recovery of spectral absolute acceleration and spectral relative velocity from their pseudo-spectral counterparts

George A. Papagiannopoulos[1], George D. Hatzigeorgiou[2] and Dimitri E. Beskos[*1,3]

[1]*Department of Civil Engineering, University of Patras, GR-26500 Patras, Greece*
[2]*Department of Environmental Engineering, Democritus University of Thrace, GR-67100 Xanthi, Greece*
[3]*Office of Theoretical and Applied Mechanics, Academy of Athens, 4 Soranou Efessiou str., GR-11527 Athens, Greece*

(Received January 17, 2012, Revised July 9, 2012, Accepted November 21, 2012)

Abstract. Design spectra for damping ratios higher than 5% have several important applications in the design of earthquake-resistant structures. These highly damped spectra are usually derived from a 5%-damped reference pseudo-acceleration spectrum by using a damping modification factor. In cases of high damping, the absolute acceleration and the relative velocity spectra instead of the pseudo-acceleration and the pseudo-velocity spectra should be used. This paper elaborates on the recovery of spectral absolute acceleration and spectral relative velocity from their pseudo- spectral counterparts. This is accomplished with the aid of correction factors obtained through extensive parametric studies, which come out to be functions of period and damping ratio.

Keywords: absolute acceleration; relative velocity; pseudo-spectral values; damping modification factor; correction factors; seismic motions

1. Introduction

Elastic response/design spectra for damping ratios higher than the typical 5% of seismic codes have several important applications in the design of earthquake-resistant structures. High damping is found in seismically isolated structures (Naeim and Kelly 1999), in structures equipped with energy dissipation devices (Soong and Constantinou 1994), as well as in the substitute structure method (Shibata and Sozen 1976) that constitutes the basis for the direct displacement-based design (Priestley *et al.* 2007) and the capacity spectrum method (ATC-40 1996).

In the aforementioned cases, highly damped response spectra are derived from the 5%-damping reference spectrum by using a damping modification factor. Until now, various expressions of this factor have been proposed and adopted, in somewhat different form, in various seismic provisions. For example, the results from Ramirez *et al.* (2002) have been implemented in NEHRP (2000), whereas the results of Bommer and Mendis (2005) have been included in the current version of EC8 (2004). More details on the implementation of damping modification factors in various seismic codes can be found in Cardone *et al.* (2004) and Hatzigeorgiou (2010).

∗Corresponding author, Professor, E-mail: d.e.beskos@upatras.gr

http://www.techno-press.org/?journal=eas&subpage=7 ISSN: 2092-7614 (Print), 2092-7622 (Online)

All proposed expressions of the damping modification factor in the literature are essentially damping dependent, even though a period dependency of that factor has also been observed in some cases. This period dependency was first recognized by Newmark and Hall (1982). The effect of additional parameters on the damping modification factor has also been studied. These parameters involve the earthquake magnitude, the source-to-site distance, the duration of ground motion and the type of soil (Bommer and Mendis 2005, Hatzigeorgiou 2010, Newmark and Hall 1982, Lin and Chang 2003, 2004, Cameron and Green 2007, Stafford *et al.* 2008). An evaluation of the accuracy of the different damping modification factors proposed in the literature has been performed in (Cardone *et al.* 2004, Lin *et al.* 2005, Hatzigeorgiou 2010).

Applying the damping modification factor to the usual 5%-damped pseudo-acceleration spectrum, one obtains a pseudo-acceleration spectrum with a different level of damping and from it the pseudo-velocity spectrum. However, when dealing with high damping, the use of spectral pseudo-acceleration or spectral pseudo-velocity may lead to errors in the calculation of the seismic design forces (Pekcan 1999, Sadek *et al.* 2000, Weitzmann *et al.* 2006, Song *et al.* 2007, Papagiannopoulos and Beskos 2010, 2011). In these cases, spectral absolute acceleration and spectral relative velocity are needed to perform the seismic design of a structure. Instead of constructing absolute acceleration and relative velocity spectra, this paper proposes a way to recover these spectra from the corresponding pseudo- counterparts by using appropriate correction factors. These correction factors can be used (a) to recover the %-damped absolute acceleration spectrum or the %-damped relative velocity spectrum from the %-damped pseudo- counterparts and (b) to recover the %-damped absolute acceleration spectrum or the %-damped relative velocity spectrum from the 5%-damped pseudo-acceleration spectrum usually found in seismic codes, where >5% is the damping ratio.

The proposed correction factors are period and damping dependent. Their mean values are determined on the basis of extensive parametric studies involving a large number of single degree of freedom systems under a large number of seismic motions. On the basis of these values, non-linear regression analyses are carried out in order to produce empirical expressions for these correction factors. It is concluded that by using those correction factors, the spectral pseudo-acceleration and spectral pseudo-velocity values can be easily transformed into spectral absolute acceleration and spectral relative velocity values, respectively.

2. Damping modification factor and ground motion database

For a linear single-degree-of-freedom (SDOF) system having a natural frequency ω or natural period T, a viscous damping ratio ξ and being subjected to ground acceleration $\ddot{u}_g(t)$, the equation of motion is given as

$$m\ddot{u}(t) + c\dot{u}(t) + ku(t) = -m\ddot{u}_g(t) \tag{1}$$

where m, c and k is the mass, damping coefficient and stiffness of the system, respectively, and $u(t)$, $\dot{u}(t)$, $\ddot{u}(t)$ are the relative displacement, relative velocity and relative acceleration, respectively. The definitions for pseudo-acceleration (PSA) and pseudo-velocity (PSV) spectra are $PSA = \omega^2 S_d$ and $PSV = \omega S_d$, respectively, where $S_d \equiv |u(t)|_{\max}$ is the displacement response spectrum. The damping modification factor n can be defined either on the basis of pseudo-acceleration or pseudo-velocity (since $PSA = \omega PSV$) and reads

$$n = \frac{PSA(T, \xi = 5\%)}{PSA(T, \xi)} = \frac{PSV(T, \xi = 5\%)}{PSV(T, \xi)} \tag{2}$$

The damping modification factors n are computed herein based on the mean values of pseudo-acceleration spectra for 866 selected accelerograms (two horizontal components of 433 accelerograms) from various earthquakes recorded worldwide. These accelerograms have been downloaded from the following on-line strong motion databases:

(a) *COSMOS: http://db.cosmos-eq.org/scripts/default.plx;*

(b) *PEER:http://peer.berkeley.edu/peer_ground_motion_database/site,*

(c) *ESD:http://www.isesd.hi.is/ESD_Local/frameset.htm*

(d) *Kiban-Kyoshin Net: http://www.kik.bosai.go.jp/*

These accelerograms have been divided into those that have been recorded at distances greater than 10 km from a fault (far-field) and those that have been recorded in the proximity of a fault, i.e., at distances less or equal to 10 km (near-field).

The far-field accelerograms have been further separated into three groups according to site conditions, i.e., AB, C and DE. The initials A to E correspond to the soil classification considered in EC8 (2004). However, site classes A and B have been grouped into one category, AB, because the results of the present paper showed a small difference between the damping modification factors of these classes if these were considered independently. The same consideration holds for site classes D and E. Thus, the site classification considered herein is AB, C and DE and corresponds to hard rock and very dense soil, stiff soil, and soft soil and alluvium, respectively. These soil classes AB, C and DE, include motions that have been recorded in profiles having an average shear wave velocity >360m/sec, 180-360 m/sec and <180 m/sec, respectively, according to EC8 (2004).

Site classes AB, C and DE include 252, 250 and 224 accelerograms, respectively. The accelerograms falling in each one of these site classes have been further subdivided into 6 moment magnitude-distance (M_w-R) bins. These bins come from the 6 possible combinations among $6.0 \le M_w \le 6.6$, $6.7 \le M_w \le 7.3$, $7.4 \le M_w \le 8.0$ and $10 \le R \le 40km$, $40 < R \le 100km$. The distance R is the Joyner-Boore distance, where available, otherwise it is the epicentral distance. This way the effect of M_w and R to the values of the damping modification factors can be studied.

The 140 near-field accelerograms have been separated according to M_w into two bins: those that have $M_w \le 6.7$ and those that have $M_w > 6.7$. This separation was done on the basis of the works of Mavroeides *et al.* (2004) and Rupakhety *et al.* (2011) who have shown that, for near-field ground motions, the normalized acceleration spectra of moderate-to-large magnitude earthquakes in the short period range are higher than those of large magnitude earthquakes. This trend is reversed at long periods. Thus, considering all near-field records together would increase the variation of individual spectra from the mean smoothed damped spectra in both short and long period ranges. The results of the present analyses reveal that a separation between moderate-to-large and large magnitude earthquakes can be done for $M_w = 6.7$.

Table 1 Far-field accelerograms, site class AB

Bin 1: $6.0 \le M_w \le 6.6,\ 10 \le R \le 40km$		
Year	Earthquake	Station
1966	Parkfield	Cholame - Shandon Array #12
1971	San Fernando	Griffith Park Observatory
		Lake Hughes Array #4
1976	Friuli	Tolmezzo
1979	Imperial Valley	Cerro Prieto
1980	Irpinia	Sturno
1980	Victoria	Cerro Prieto
1983	Coalinga	Parkfield - Fault Zone 6
		Parkfield - Gold Hill 3E
1984	Morgan Hill	Corralitos
1986	N. Palm Springs	Joshua Tree
		Santa Rosa Mountain
1987	Whittier Narrows	CalTech Seismic Station
1992	Big Bear	Silent Valley - Poppet Flat
1999	Chi-Chi	CHY028
		TCU073
		TCU051
2000	South Iceland	Flagbjarnarholt
		Thjorsarbru
2002	Avej	Bakhshdari
2003	Bingol	Bayindirlik Murlugu
2008	Olfus	Hveragerdi
2008	Olfus	SelfossCity Hall
2009	Tokai	Shizuoka Prefecture
2011	Fukushima	Takahagi

Bin 3: $6.7 \le M_w \le 7.3,\ 10 \le R \le 40km$		
Year	Earthquake	Station
1978	Tabas	Dayhook
1979	Montenegro	Petrovac-Hotel Oliva
		Ulcinj-Hotel Olimpic
1980	Irpinia	Bagnoli-Irpino
		Calitri
		Rionero In Vulture
		Sturno
1983	Kefallinia	OTE Building
1989	Loma Prieta	San Jose - Santa Teresa Hills
		Hollister - South & Pine
		Gilroy Array #6
		Fremont - Mission San Jose
1992	Cape Mendocino	Fortuna - Fortuna Blvd
		Shelter Cove Airport
1992	Landers	Joshua Tree
1994	Northridge	Station USC 059, Burbank
		Mt. Wilson, Caltech station
1999	Duzce	Lamont 362
		LDEO Station No. C0375
		LDEO Station No. C1061
		LDEO Station No. D0531
		Mudurnu
1999	Hector Mine	Hector
		Joshua Tree
2003	Miyagi-oki	Touwa

Bin 2: $6.0 \le M_w \le 6.6,\ 40 < R \le 100km$		
Year	Earthquake	Station
1976	Friuli	Barcis
1983	Coalinga	Parkfield - Cholame 2E
		Parkfield - Cholame 12W
1980	Irpinia	Brienza
		Tricarico

Bin 4: $6.7 \le M_w \le 7.3,\ 40 < R \le 100km$		
Year	Earthquake	Station
1978	Tabas	Boshroyeh
1979	Montenegro	Titograd-Seismoloska Stanica
		Hercegnovi Novi-Pavicic Sch.
1980	Irpinia	Arienzo
		Brienza

Table 1 Continued

1986	N. Palm Springs	Rancho Cucamonga - FF	1986	Vrancea	Torre del Greco
		Temecula - 6th & Mercedes			Vrancioaia
		Winchester Bergman Ran	1989	Loma Prieta	Yerba Buena Island
1992	Big Bear	Joshua Tree			Sunol - Forest Fire Station
		Temecula - 6th & Mercedes			Rincon Hill
		Winchester Bergman Ran			Pacific Heights
1992	Erzincan	Tercan-Meteoroji Mudurlugu			Bear Valley #5, Callens Ranch
		Refahiye-Kaymakamlik Binasi			Bear Valley #7, Pinnacles
1995	Kozani	Florina-Cultural Center			Monterey City Hall
		Kastoria-OTE Building			Presidio
1997	Umbria Marche	Peglio			APEEL 7 - Pulgas
1999	Chi-Chi	CHY041	1992	Landers	Silent Valley - Poppet Flat
		CHY052			Twentynine Palms
		CHY062	1995	Kobe	MZH
		CHY087	1999	Duzce	Sakarya
		CHY102	1999	Hector Mine	Heart Bar State Park
2000	South Iceland	Sultartangastifla			Twentynine Palms
		Sigolduvirkjun	2003	Miyagi-Oki	MYG011 Oshika
		Sigoldustifla			IWTH23 Kamaishi
		Thorlakshofn	2005	Off. E. Miyagi	MYG011

Bin 5: $7.4 \le M_w \le 8.0$, $10 \le R \le 40km$			Bin 6: $7.4 \le M_w \le 8.0$, $10 \le R \le 40km$		
Year	Earthquake	Station	Year	Earthquake	Station
1985	Michoachan	Caleta de Campos	1978	Miyagi-oki	Ofunato Bochi*
1985	Chile	Quintay	1985	Chile	Zapallar
		Valparaiso			Papudo
1999	Kocaeli	Goynuk			Rapel
1999	Chi-Chi	TCU109	1999	Chi-Chi	CHY081
		CHY010	1999	Izmit	Gebze-Arcelik
		CHY042			HWA022
		CHY052			HWA034
		HWA038			Heybeliada-Senatoryum
		TCU105			HWA029
		TCU088			HWA005
					Gebze-Tubitak Marmara
			1999	Kocaeli	Bursa Sivil
					Mecidiyekoy
			2001	Southern Peru	Moquegua

Table 2 Far-field accelerograms, site class C

Bin 1: $6.0 \le M_w \le 6.6$, $10 \le R \le 40km$			Bin 3: $6.7 \le M_w \le 7.3$, $10 \le R \le 40km$		
Year	Earthquake	Station	Year	Earthquake	Station
1971	San Fernando	Castaic Old Ridge Route	1988	Spitak	Gukasian
1978	Volvi	Thessaloniki-City Hotel			Fremont Emerson Court
		El Centro Array #1			Gilroy Array #4
1979	Imperial Valley	Parachute Test site			Hollister Differential Array
		Westmoreland Fire Station			Palo Alto 1900
1979	Imperial Valley	Superstition Mountain	1989	Loma Prieta	Sunnyvale Colton Avenue
		Chihuahua			Gilroy Array #1
1980	Victoria	Sahop Casa Flores			Halls Valley
1981	Alkionides	Korinthos-OTE Building			San Jose, Santa Teresa Hills
		Parkfield, Fault zone 16			Desert Hot Springs
1983	Coalinga	Parkfield, Fault zone 16			Morango Valley
		Vineyard Cany 1E	1992	Landers	N. Palm Springs Fire Station
		Capitola			Joshua Tree Fire Station
		Gilroy Array #2	1994	Arthurs Pass	Arthurs Pass, Police Station
1984	Morgan Hill	Gilroy Array #7			Figueroa Street 5921
		Hollister Differential Array #4			12520 Mulholland
1986	Chalfant Valley	Bishop - Paradise Lodge	1994	Northridge	Century City CC North
1986	N. Palm Springs	Hemet Stetson Avenue			Westmoreland
		Palm Springs Airport			Temple & Hope
1987	Whittier Narrows	Arleta Nordhoff			Kakowaga
		Santa Fe Springs	1995	Kobe	Shin-Osaka
1992	Big Bear	Sage - Fire Station			Abeno
1997	NW Kagoshima	KGS005 Miyanojoh	1999	Duzce	Bayindirlik Iskan Mudurlugu
1998	Adana	Ceyhan-Tarim Ilce Mudurlugu			LDEO Station No. C1062 FI
2001	Geiyo	HRS 019 Kure	2000	Western Tottori	SMN003 Yokota
Bin 2: $6.0 \le M_w \le 6.6$, $40 < R \le 100km$			Bin 4: $6.7 \le M_w \le 7.3$, $40 < R \le 100km$		
Year	Earthquake	Station	Year	Earthquake	Station
1973	Te Aroha	Atene	1988	Te Anau	Te Anau - Fire Station
1979	Imperial Valley	Coachella, Canal Station 4			Bear Valley #10
		Parkfield, Cholame 8W	1989	Loma Prieta	Bear Valley #12
1983	Coalinga	Parkfield, Fault Zone 1			Emeryville 6363 Christie
		Parkfield, Cholame 1			SF International Airport
1984	Morgan Hill	Apeel 1E Hayward	1992	Cape Mendocino	Eureka – Myrtle & West

Table 2 Continued

1984	Morgan Hill	Los Banos	1992	Landers	Amboy
1986	Palm Springs	Anza Fire Station			Indio - Coachella Canal
		Colton Vault	1994	Northridge	Santa Fe Springs - E. Joslin
1987	Whittier Narrows	Calabasas			Lakewood - Del Amo Blvd
		Malibu Point Dome			Castaic Old Ridge Route
		Newhall			Lake Hughes 12A
1992	Big Bear	Hemet Stetson Avenue Fire St.			Point Mugu – Laguna Peak
		Phelan Wilson Ranch Road			Downey - County Maint. Bldg
		Yermo Fire Station			Terminal Island - Fire St. 111
		Wrightwood Neilson Ranch	1999	Hector Mine	Amboy
1993	Ormond	Gisborne, Kaiti Hill			Baker Fire Station
1999	Chi-Chi	CHY015			Big Bear Lake - Fire Station
		CHY026	2000	Western Tottori	HRS001 Takano
		CHY033			HRS002 Tohjoh
		CHY039			OKY005 Ochiai
		CHY092	2003	Miyagi-oki	Ichinoseki
		CHY111			MYGHO5 Onoda
2001	Geiyo	EHM003 Tokyo	2004	Hokkaido	HKD074 Nosappu
2004	Chuetsu	NIG024 Yasuduka	2007	Noto Hanto	ISK004
Bin 5: $7.4 \le M_w \le 8.0,\ 10 \le R \le 40km$			Bin 6: $7.4 \le M_w \le 8.0,\ 10 \le R \le 40km$		
Year	Earthquake	Station	Year	Earthquake	Station
1985	Chile	Llolleo	1968	Tokachi Oki	Hachinohe Harbor*
1999	Chi-Chi	TCU061	1974	Peru Coast	Casa Huaco, Las Gardenias*
		TCU0110	1985	Chile	Melpilla
		TCU0111	1990	Manjil	Abhar
		TCU0123			Qazvin
1999	Kocaeli	Duzce 180 ERD			Rudsar
		Iznik-Karayollari Sefligi			Tonekabun*
2007	Ica Pisca	ICA2	1999	Kocaeli	Atakoy
					Bursa Tofas
					Fatih Tomb
					IstanbulZeytinburnu
					IstanbulK.M.Pasa
			2001	El Salvador	Observatorio
					Santa Tecla
			2002	Denali	Taps Pump Station 12*
			2003	Tokachi-oki	HKD092 Ikeda*
					HKD100 Hiroo

Table 3 Far-field accelerograms, site class DE

Bin 1: $6.0 \le M_w \le 6.6,\ 10 \le R \le 40km$

Year	Earthquake	Station
1966	Parkfield	Cholame 8W
1979	Imperial Valley	Calexico - Fire Station
		El Centro - Keystone Rd
		El Centro - Pine Union School
1984	Morgan Hill	Gilroy Array Station 2
		Gilroy Array Station 3
1987	Whittier Narrows	1307 S Orange Ave
		Bell Gardens - Grant LDS Church
		Santa Fe Springs - Lakeview Sch.
		Hacienda Heights - 16750 Colima
		Vernon City School
		Los Angeles - Fire Station 50
		Downey - South Middle School
		Glendale - Fremont Elem School
		Los Angeles - 116th St School
		Inglewood - Union Oil Yard
		Westminister Presbyterian Church
1987	Superstition Hills	Westmorland - Fire Station
		Plaster City - Warehouse
1999	Chi-Chi	TCU079
		CHY101
		CHY047
		TCU065
2004	Parkfield	Cholame 5W
2007	Chuetsu Oki	Kashiwazaki

Bin 2: $6.0 \le M_w \le 6.6,\ 40 < R \le 100km$

Year	Earthquake	Station
1971	San Fernando	Whittier Narrows Dam
1979	Imperial Valley	Coachella - Canal Station 4
		TCU112
		TCU113
1984	Morgan Hill	Capitola
1987	Whittier Narrows	Canoga Park
		Sulphur Springs School
		White Oak Covenant Church
1990	Weber	Woodville - Post Office

Bin 3: $6.7 \le M_w \le 7.3,\ 10 \le R \le 40km$

Year	Earthquake	Station
1989	Loma Prieta	Hollister - City Hall Annex
		Gilroy Array Station 7
		Redwood City - Array Station 1
		Sunnyvale - Salsman Residence
1992	Landers	Desert Hot Springs - New Fire St.
		Palm Springs - Airport
		Yermo- Fire Station
1994	Northridge	Pacific Palisades - Fire Station 23
		Century City Country Club North
		Santa Monica City Hall Grounds
		Hollywood Storage Bldg Grounds
		McBride School
		Sulphur Springs School
		Fremont Elem School
		Obregon Park
		Laurel Childrens Center
		Pico & Sentous
		Los Angeles - City Terrace
		Vernon City School
		Baldwin Hills

Bin 4: $6.7 \le M_w \le 7.3,\ 40 < R \le 100km$

Year	Earthquake	Station
1989	Loma Prieta	APEEL 2 - Redwood City
		Foster City - Menhaden Court
		Treasure Island
		Hayward - Muir School
		San Francisco - Airport
		Oakland - Outer Harbor Wharf
1992	Landers	Hemet Fire Station
		Amboy
		Fort Irwin
1994	Northridge	Carson - Water St
		Hawthorne LDS Church
		Union Oil Yard
		Downey - County Maint. Bldg
		Downey - South Middle School

Table 3 Continued

1999	Chi-Chi	CHY039	1994	Northridge	Camarillo - Lake Hughes Array
		TCU141			Lakeview School
		CHY036			Mira Catalina School
		CHY047			Lakewood - Mae Bayer Park
		CHY082			Terminal Island - Fire Station 111
		CHY025	2003	Miyagi-oki	Kamaishi
		TCU051			
		TCU050			
		TCU061			
		TCU118			
		TCU059			
		TCU140			
Bin 5: $7.4 \le M_w \le 8.0,\ 10 \le R \le 40km$			Bin 6: $7.4 \le M_w \le 8.0,\ 10 \le R \le 40km$		
Year	Earthquake	Station	Year	Earthquake	Station
1985	Chile	Vina del Mar	1985	Chile	Ventanas
		Valparaiso el Almendral			Llayllay
1999	Chi-Chi	CHY101	1985	Michoachan	SCT*
		TCU063	1999	Chi-Chi	CHY054
		TCU061			CHY078
		CHY104			CHY107
		CHY036			CHY008
		CHY010			HWA051
		TCU036			HWA005
		TCU042			CHY015
		TCU123			HWA019
			2001	El Salvador	Zacatecoluca
					La Libertad
					Presa 15 De Septiembre Dam
			2003	Tokachi-Oki	HKD066 Shibetsu*

Table 4 Near-field accelerograms

Bin 1: $M_w \le 6.7,\ 0 \le R \le 10km$			Bin 2: $M_w > 6.7,\ 0 \le R \le 10km$		
Year	Earthquake	Station	Year	Earthquake	Station
1966	Parkfield	Cholame 2WA	1976	Gazli	Karakyr
1971	San Fernando	Pacoima Dam	1977	Bucharest	Bucharest Research Institute
1978	Coyote Lake	Gilroy Array 6	1978	Tabas	Tabas
1979	Imperial Valley	El Centro Array #4	1989	Loma Prieta	Corralitos
		El Centro Array #5			Lexington Dam - Left Abutment
		El Centro Array #6			Los Gatos Presentation Center
		El Centro Array #7			Saratoga - Aloha Ave
		El Centro Array #8	1992	Landers	Lucerne Valley
		Bonds Corner	1992	Cape Mendocino	Cape Mendocino

Table 4 Continued

1979	Imperial Valley	Meloland Route 8 Overpass	1992	Cape Mendocino	Petrolia
		Holtville- Post Office	1995	Kobe	Takatori
		Differential Array, Dogwood RD			Port Island
1980	Mexicali Valley	Cerro Prieto			Kobe University
		Victoria			Takarazuka
1984	Morgan Hill	Coyote Lake Dam			KJMA
1986	Palm Springs	North Palm Springs - Post Office	1999	Kocaeli	Yarimca - Petkim
1987	Superstition Hill	Parachute Test Site			Izmit-Meteoroloji Istasyonu
1992	Erzincan	Erzincan			Sakarya
1994	Northridge	Tarzana - Cedar Hill Nursery	1999	Duzce	Duzce-Meteoroloji Mudurlugu
		Sepulveda VA Hospital	1999	Chi-Chi	TCU072
		Rinaldi Receiving Station			TCU074
		Los Angeles Dam			TCU075
		Jensen Filtration Plant Generator			TCU076
		Sylmar - Converter Station			TCU078
		Sylmar - Converter Station East			TCU120
		Simi Valley			TCU065
		Sylmar - County Hospital			TCU067
		Pacoima- Kagel Canyon			CHY101
		Newhall – L. A. County Fire St.			CHY028
		White Oak Covenant Church			TCU055
		Newhall - Pico Canyon			TCU082
1995	Aigion	AEG			TCU052
2011	New Zealand	Lyttelton Port Company			TCU102
		Christchurch Resthaven			TCU068
					TCU103
					TCU051

It should be noted that in contrast to the large number of far-field ground motion recordings which permits a site classification, such a classification is not possible for the near-field ones due to the small number of the corresponding recordings.

Details about the far-field accelerograms that correspond to site classes AB, C and DE, are shown in Tables 1-3, respectively, whereas for the near-field accelerograms are given in Table 4. In each one of Tables 1-3, the 6 bins associated with the separation of the accelerograms according to M_w and R are found. In Table 4, the near-field accelerograms have been separated into two bins according to only M_w. It should be noted that those accelerograms denoted with an asterisk (*) in Tables 1-3 have been recorded at distances greater than 100 km. Moreover, the accelerogram from the Bucharest, 1977 earthquake, although it has been recorded far from the fault, it has been considered in the category of near-field ground motions because it exhibits the characteristic pulse of this kind of motions.

Mean pseudo-acceleration and pseudo-velocity spectra of the far- and near-field accelerograms and for a family of SDOF systems having periods from 0.01 to 5 sec in steps of 0.005 sec and a fixed damping ratio of 5, 8, 10, 15, 20, 25, 30, 40, 50 % are first constructed. Using these spectra, the mean values of the damping modification factor n on the basis of Eq. (2) are obtained.

3. Absolute spectra and corrections factors

Considering again Eq. (1), the definitions for absolute acceleration (SA) and relative velocity (SV) spectra are $SA = \left|\ddot{u}(t) + \ddot{u}_g(t)\right|_{\max}$ and $SV = \left|\dot{u}(t)\right|_{\max}$, respectively. Next, the correction factors n_a and n_v that can be used to recover the ξ%-damped absolute acceleration spectrum or the ξ%-damped relative velocity spectrum from the ξ%-damped pseudo- counterparts whenξ>5% are defined as

$$n_a = \frac{SA(T,\xi)}{PSA(T,\xi)} \tag{3a}$$

$$n_v = \frac{SV(T,\xi)}{PSV(T,\xi)} \tag{3b}$$

Using the mean absolute acceleration, pseudo-acceleration, relative velocity and pseudo-velocity spectra constructed for periods from 0.01 to 5 sec in steps of 0.005 sec and for damping ratios 5, 8, 10, 15, 20, 25, 30, 40, 50 %, one finds the mean values of the correction factors n_a and n_v. Plots of the mean values of these correction factors for the cases of (1) far-field motions having $6.7 \leq M_w \leq 7.3$, $10 \leq R \leq 40$ km at site class C (Bin 3 at Table 2) and (2) near-field motions having $M_w \leq 6.7$ (Bin 1 at Table 4)are shown in Figs. 1 and 2. Similar figures can be constructed for the rest of far- and near-field motions but are not shown herein due to space limitations.

It should be noted that n_a and n_v also reveal the difference between absolute acceleration and pseudo-acceleration and between relative velocity and pseudo-velocity, respectively. More specifically, the values of n_a in Fig. 1 reveal that for structures with small amount of damping, i.e., $< 15\%$, the peak absolute acceleration can be approximated by the peak pseudo-acceleration with good accuracy. However, for larger than 15% damping ratio, this approximation is inaccurate. The values of n_v in Fig. 2 reveal that relative velocity can be greater or lesser than the pseudo-velocity depending on the period and the damping ratio.

On the basis of the mean values of n_a and n_v, nonlinear regression analyses are conducted using the Table Curve 3D (2002)scientific software and the following empirical equation for n_a and n_v is found:

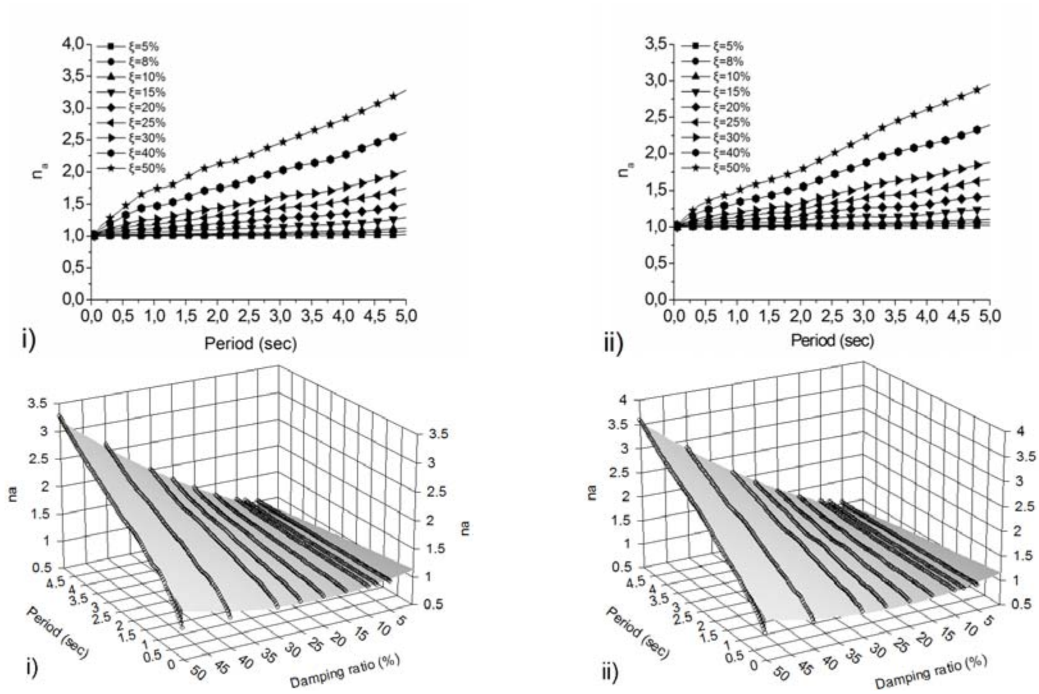

Fig. 1 Mean values of n_a for (i) far-field, $6.7 \leq M_w \leq 7.3$, $10 \leq R \leq 40$ km, site class C and (ii) near-field, $M_w \leq 6.7$ motions

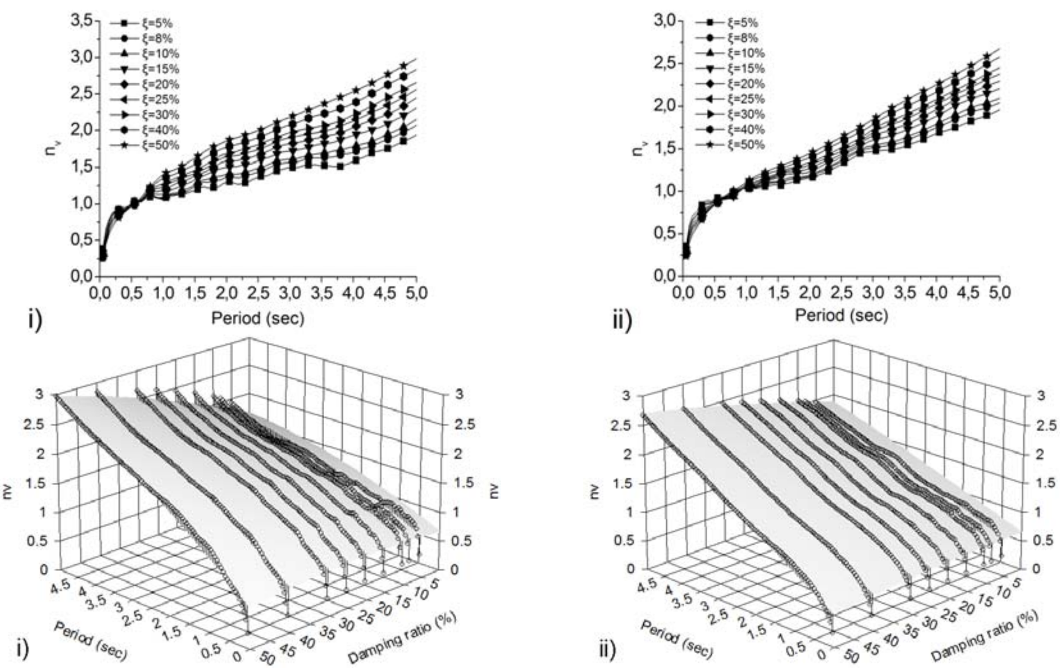

Fig. 2 Mean values of n_v for (i) far-field, $6.7 \leq M_w \leq 7.3$, $10 \leq R \leq 40$ km, site class C and (ii) near-field, $M_w \leq 6.7$motions

$$n_{a,v} = a + bT + c\xi + dT^2 + e\xi^2 + f\xi T \tag{4}$$

Parameters a - f of Eq. (4) satisfy the constraint n_α=1.00-1.10 for $\xi = 5\%$ and 0.05≤T≤5.0 sec. The criterion for the selection of this equation is the minimum absolute residual error using the Pearson VII limit (Table Curve 3D 2002), i.e., minimum sum of $\ln\left[\sqrt{1+residual^2}\right]$. The values for the parameters a - f as well as the correlation coefficients r^2 and the standard deviations (sd) of Eq. (4) for the cases of n_a and n_v are shown in Tables 5-6, respectively, for the far- and near-field ground motions considered herein. The bins mentioned in Tables 5 and 6 correspond to the M_w-R bins of Tables 1-4. Three-dimensional plots using the empirical model of Eq. (4) and the mean values of these correction factors for (i) far-field motions having 6.7≤M_w≤ 7.3, 10≤R≤40 km at site class C and (ii) near-field motions having M_w≤6.7 are also shown in Figs.1 and 2.

In the following, the correction factors λ_a and λ_v that can be used to recover the ξ%-damped absolute acceleration spectrum or the ξ%-damped relative velocity spectrum from the 5%-damped pseudo- counterparts are defined as

$$\lambda_a = SA(T,\xi)/PSA(T,5\%) \tag{5a}$$

$$\lambda_v = SV(T,\xi)/PSV(T,5\%) \tag{5b}$$

Table 5 Parameters, correlation coefficients and standard deviations of Eq.(4) for n_a

Type of motion		a	b	c	d	e	f	r^2	sd
Far-field, Site AB	Bin 1	1.1581	-0.1616	-0.0161	0.0150	0.0003	0.0201	0.999	0.032
	Bin 2	1.2108	-0.1581	-0.0173	0.0151	0.0004	0.0105	0.994	0.043
	Bin 3	1.2130	-0.1432	-0.0214	0.0124	0.0005	0.0122	0.995	0.047
	Bin 4	1.0574	-0.0153	-0.0096	-0.0076	0.0003	0.0065	0.986	0.049
	Bin 5	1.0829	-0.0224	-0.0120	-0.0051	0.0004	0.0058	0.987	0.043
	Bin 6	1.1832	-0.1038	-0.0190	0.0051	0.0004	0.0100	0.994	0.041
Far-field, Site C	Bin 1	1.2105	-0.1753	-0.0211	0.0145	0.0004	0.0171	0.997	0.045
	Bin 2	1.2355	-0.1968	-0.0221	0.0203	0.0004	0.0164	0.997	0.040
	Bin 3	1.1305	-0.0720	-0.0150	2.62e-05	0.0004	0.0089	0.994	0.039
	Bin 4	1.0710	-0.0080	-0.0148	-0.0126	0.0004	0.0097	0.992	0.050
	Bin 5	1.0488	-0.0167	-0.0065	-0.0024	0.0002	0.0036	0.982	0.030
	Bin 6	1.1373	-0.0399	-0.0177	-0.0069	0.0004	0.0080	0.988	0.048
Far-field, Site DE	Bin 1	1.1356	-0.0865	-0.0175	0.0017	0.0004	0.0124	0.997	0.036
	Bin 2	1.2120	-0.1442	-0.0223	0.0096	0.0005	0.0138	0.994	0.056
	Bin 3	1.1788	-0.0948	-0.0203	-0.0014	0.0004	0.0120	0.993	0.049
	Bin 4	1.1612	-0.0867	-0.0191	0.0004	0.0004	0.0107	0.994	0.044
	Bin 5	1.0726	-0.0375	-0.0069	0.0005	0.0002	0.0040	0.984	0.029
	Bin 6	1.0849	-0.0404	-0.0099	-0.0007	0.0003	0.0054	0.990	0.031
Near-field	Bin 1	1.1257	-0.0776	-0.0128	0.0024	0.0003	0.0083	0.994	0.032
	Bin 2	1.0836	-0.0472	-0.0080	0.0019	0.0002	0.0044	0.991	0.024

Table 6 Parameters, correlation coefficients and standard deviations of Eq. (4) for n_v

Type of motion		a	b	c	d	e	f	r^2	sd
Far-field, Site AB	Bin 1	0.5885	0.6735	0.0110	0.0209	-0.0002	0.0052	0.998	0.061
	Bin 2	0.8281	0.0846	0.0069	0.0368	-0.0001	0.0051	0.975	0.097
	Bin 3	0.6943	0.2776	0.0090	0.0249	-0.0001	0.0046	0.983	0.103
	Bin 4	0.7526	0.3351	0.0066	-0.0388	-0.0001	0.0040	0.932	0.104
	Bin 5	0.7739	0.2029	0.0042	-0.0133	-6.92e-05	0.0042	0.947	0.090
	Bin 6	0.6899	0.3199	0.0049	-0.0132	-9.63e-05	0.0052	0.980	0.083
Far-field, Site C	Bin 1	0.5992	0.4281	0.0131	0.0372	-0.0002	0.0051	0.994	0.085
	Bin 2	0.5556	0.4006	0.0109	0.0416	-0.0002	0.0044	0.995	0.074
	Bin 3	0.6728	0.3226	0.0078	-0.0255	-0.0002	0.0052	0.975	0.080
	Bin 4	0.6452	0.4824	0.0110	-0.0458	-0.0002	0.0049	0.984	0.074
	Bin 5	0.7315	0.2140	-0.0029	-0.0260	-1.37e-05	0.0030	0.926	0.068
	Bin 6	0.6981	0.3003	0.0049	-0.0324	-0.0001	0.0060	0.971	0.080
Far-field, Site DE	Bin 1	0.6000	0.4901	0.0095	-0.0170	-0.0001	0.0042	0.991	0.070
	Bin 2	0.6890	0.3530	0.0130	0.0182	-0.0001	0.0048	0.982	0.116
	Bin 3	0.5988	0.3773	0.0083	-0.0248	-0.0002	0.0075	0.985	0.083
	Bin 4	0.6192	0.3593	0.0094	-0.0252	-0.0002	0.0068	0.980	0.089
	Bin 5	0.8307	0.1523	-0.0040	-0.0121	1.45e-06	0.0024	0.943	0.054
	Bin 6	0.6863	0.3148	0.0014	-0.0354	-5.21e-05	0.0032	0.960	0.068
Near-field	Bin 1	0.6526	0.2625	0.0019	-0.0040	-7.82e-05	0.0037	0.986	0.057
	Bin 2	0.7887	0.1325	-0.0025	-0.0038	-1.18e-05	0.0024	0.947	0.059

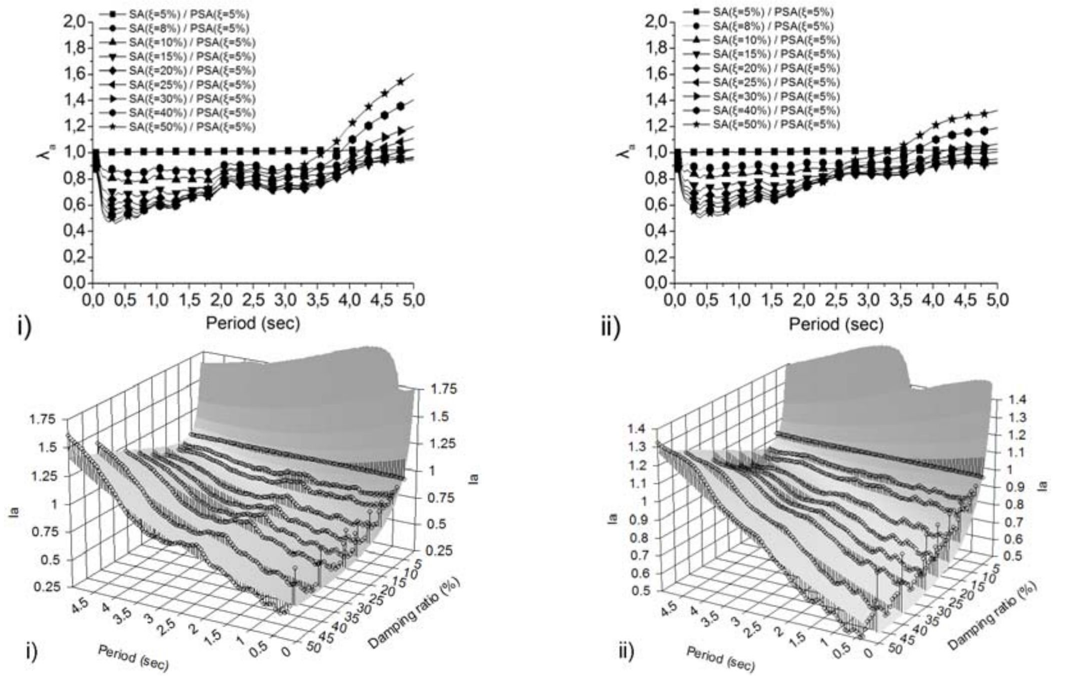

Fig. 3 Mean values of λ_a for (i) far-field, $6.7 \le M_w \le 7.3$, $10 \le R \le 40$ km, site class C and (ii) near-field, $M_w \le 6.7$ motions

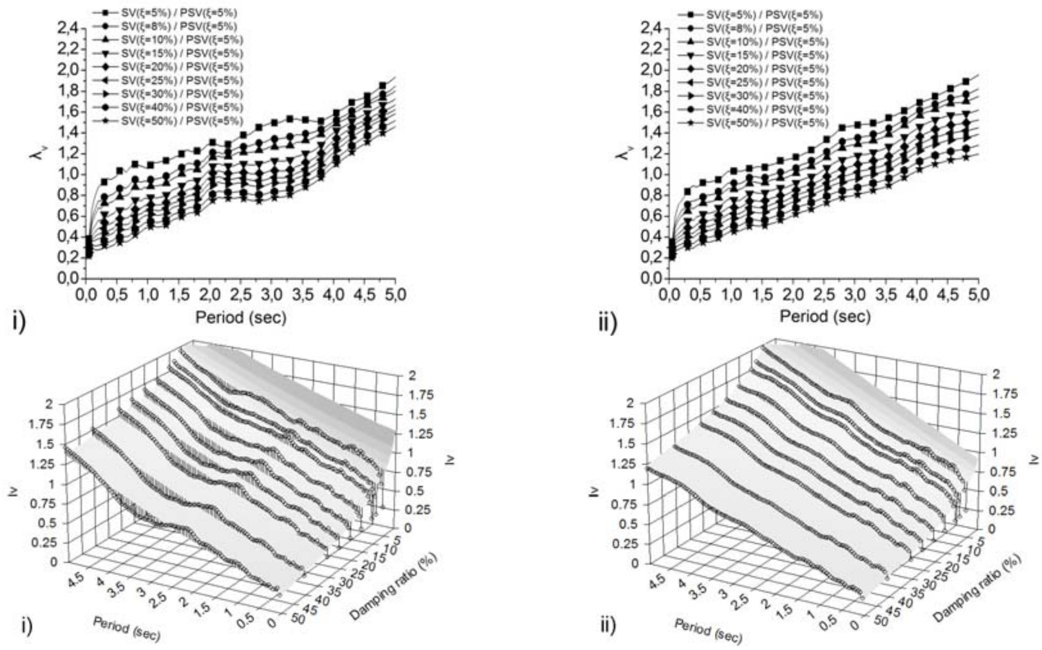

Fig. 4 Mean values of λ_v for (i) far-field, $6.7 \leq M_w \leq 7.3$, $10 \leq R \leq 40$ km, site class C and (ii) near-field, $M_w \leq 6.7$ motions

Table 7 Parameters, correlation coefficients and standard deviations of Eq. (6) for λ_a

Type of motion		a	b	c	d	e	f	r^2	sd
Far-field, Site AB	Bin 1	2.8990	-0.4368	-1.3493	0.0216	0.1881	0.1976	0.980	0.063
	Bin 2	2.6681	-0.3630	-1.1242	0.0309	0.1447	0.1098	0.913	0.067
	Bin 3	2.8370	-0.3631	-1.3006	0.0249	0.1813	0.1330	0.952	0.061
	Bin 4	2.2476	-0.1078	-0.9463	-0.0017	0.1305	0.0614	0.891	0.047
	Bin 5	2.0939	-0.0809	-0.8229	0.0050	0.1082	0.0328	0.819	0.062
	Bin 6	2.4842	-0.2213	-1.0646	0.0160	0.1461	0.0760	0.865	0.065
Far-field, Site C	Bin 1	2.6858	-0.2684	-1.2535	0.0045	0.1786	0.1787	0.957	0.059
	Bin 2	2.9792	-0.5142	-1.3198	0.0501	0.1782	0.1503	0.938	0.083
	Bin 3	2.4882	-0.2735	-1.0317	0.0220	0.1374	0.0855	0.890	0.061
	Bin 4	2.5673	-0.1739	-1.1915	-0.0030	0.1724	0.0100	0.917	0.059
	Bin 5	1.9521	-0.1318	-0.6449	0.0209	0.0741	0.0166	0.903	0.050
	Bin 6	2.4460	-0.2003	-1.0338	0.0123	0.1403	0.0700	0.840	0.065
Far-field, Site DE	Bin 1	2.8123	-0.4067	-1.2468	0.0267	0.1688	0.1509	0.951	0.069
	Bin 2	2.7031	-0.3232	-1.2016	0.0257	0.1693	0.1058	0.915	0.066
	Bin 3	2.5153	-0.2961	-1.0480	0.0202	0.1388	0.1015	0.920	0.057
	Bin 4	2.8088	-0.3155	-1.2879	0.0171	0.1798	0.1194	0.927	0.064
	Bin 5	1.8795	-0.0350	-0.6597	0.0020	0.0782	0.0159	0.913	0.044
	Bin 6	2.2820	-0.2362	-0.8739	0.0232	0.1097	0.0640	0.889	0.054
Near-field	Bin 1	2.1298	-0.1827	-0.7875	0.0086	0.0983	0.0726	0.904	0.046
	Bin 2	2.0324	-0.1567	-0.7125	0.0121	0.0842	0.0517	0.932	0.036

Table 8 Parameters, correlation coefficients and standard deviations of Eq.(6) for λ_v

Type of motion		a	b	c	d	e	f	r^2	sd
Far-field, Site AB	Bin 1	0.9743	0.7970	-0.1383	0.0350	-0.0135	-0.1112	0.998	0.047
	Bin 2	1.4549	0.0148	-0.3285	0.0532	0.0103	-0.0009	0.976	0.073
	Bin 3	1.1996	0.2452	-0.2485	0.0445	0.0060	-0.0281	0.988	0.066
	Bin 4	1.3866	0.2464	-0.3347	-0.0210	0.0111	0.0058	0.940	0.075
	Bin 5	1.3032	0.1807	-0.3085	0.0008	0.0131	-0.0160	0.910	0.089
	Bin 6	1.3386	0.2723	-0.3622	0.0088	0.0238	-0.0266	0.964	0.080
Far-field, Site C	Bin 1	0.9136	0.6812	-0.1717	0.0199	0.0043	-0.1078	0.992	0.066
	Bin 2	1.2125	0.3665	-0.2981	0.0810	0.0215	-0.0948	0.993	0.070
	Bin 3	1.3146	0.1480	-0.2702	0.0087	-0.0011	0.0090	0.967	0.067
	Bin 4	1.2868	0.3875	-0.3022	-0.0261	0.0055	0.0010	0.989	0.045
	Bin 5	1.4523	0.0944	-0.4226	0.0030	0.0293	-0.0067	0.939	0.061
	Bin 6	1.4074	0.1240	-0.3448	8.04e-05	0.0115	0.0193	0.942	0.077
Far-field, Site DE	Bin 1	1.1301	0.3301	-0.1608	0.0244	-0.0178	-0.0171	0.993	0.054
	Bin 2	1.2249	0.3759	-0.2430	0.0402	0.0110	-0.0772	0.980	0.086
	Bin 3	1.0246	0.2317	-0.0946	0.0080	-0.0327	0.0045	0.984	0.058
	Bin 4	1.3435	0.1675	-0.3307	0.0053	0.0086	0.0312	0.977	0.068
	Bin 5	1.3913	0.1703	-0.3967	-0.0073	0.0256	-0.0169	0.985	0.031
	Bin 6	1.4300	0.1168	-0.3828	0.0017	0.0183	0.0123	0.968	0.054
Near-field	Bin 1	0.9469	0.2705	-0.1204	0.0026	-0.0171	-0.0201	0.992	0.035
	Bin 2	1.2906	0.0694	-0.2935	0.0084	0.0071	0.0064	0.984	0.032

Using the mean absolute acceleration, pseudo-acceleration, relative velocity and pseudo-velocity spectra constructed for periods from 0.01 to 5 sec in steps of 0.005 sec and for damping ratios 5, 8, 10, 15, 20, 25, 30, 40, 50 %, the mean values of the correction factors λ_a and λ_v are found.The mean values of λ_a and λ_v for far-field motions having $6.7 \le M_w \le 7.3$, $10 \le R \le 40$km at site class C and for near-field motions having $M_w \le 6.7$ are shown in Figs.3-4. Similar figures can be constructed for the rest of far- and near-field motions but are not shown herein due to space limitations. From Eqs. (2) and (3), it can be easily shown that $\lambda_a = n_a / n$ and $\lambda_v = n_v / n$.

On the basis of the mean values of λ_a and λ_v, nonlinear regression analyses are performed using the Table Curve 3D (2002) scientific software and the following empirical equation for λ_a and λ_v is found

$$\lambda_{a,v} = a + bT + c\ln\xi + dT^2 + e(\ln\xi)^2 + fT\ln\xi \tag{6}$$

Parameters a - f of Eq. (6) satisfy the constraint λ_α=1.00-1.10 for $\xi = 5\%$ and $0.05 \le T \le 5.0$ sec. The criterion for the selection of this equation is the minimum absolute residual error using the Pearson VII limit (Table Curve 3D 2002), i.e., minimum sum of $\ln\left[\sqrt{1+residual^2}\right]$. The values for the parameters a - f as well as the correlation coefficients r^2 and the standard deviations (sd) of Eq. (6) for the cases of λ_a and λ_v are shown in Tables 7 and 8, respectively, for the far- and near-field ground motions considered herein. The bins mentioned in Tables 7 and 8 correspond to M_w-R bins of Tables 1 and 4. Three-dimensional plots using the empirical model of Eq. (6) and the mean values of these correction factors for (i) far-field motions having $6.7 \leq M_w \leq 7.3$, $10 \leq R \leq 40$ km at site class C and (ii) near-field motions having $M_w \leq 6.7$ are also shown in Figs. 3 and 4.

4. Discussion

The calculation of the correction factors proposed herein is based on mean values of response spectra. Using mean plus one deviation spectral values for the derivation of these factors (Lin and Chang 2003) may produce non-conservative results and unsafe seismic design (Bommer and Mendis 2005).

From the results of Tables 5-8 it can be said that the correction factors used to recover the absolute acceleration and the relative velocity from their pseudo-spectral counterparts depend on earthquake magnitude, site class and site-to-source distance. These correction factors are found to be functions of damping ratio and period.

In Tables 5 and 6, the parameters of the empirical equations for n_a and n_v are found to give correlation coefficients r^2 of the order of at least 98% and 93%, respectively. The order of the correlation coefficients depends on the combination among earthquake magnitude, site class and site-to-source distance. This means that the variability of the data is correctly accounted by the empirical equation. On the other hand, the parameters of the empirical equations for λ_a and λ_v in Tables 7 and 8 are found to give correlation coefficients r^2 of the order of at least 82% and 94%, respectively. Similarly as before, the order of the correlation coefficients depends on the combination among earthquake magnitude, site class and site-to-source distance.

In praxis, considering the values of the correlation coefficients of Tables 6 and 8, the use of the correction factors n_v and λ_v renders the recovery of relative velocity from pseudo-velocity at any value of damping accurate. Accuracy is also maintained in the case that the absolute acceleration is recovered from pseudo-acceleration at any value of damping by using the correction factor n_a, as the correlation coefficients in Table 5 reveal. However, from the correlation coefficients of Table 7, the recovery of absolute acceleration from the 5%-damped pseudo-acceleration by using the correction factor λ_a can be accurate or accurate enough depending on the period and the damping ratio.

On the other hand, it should be noted that the results obtained by the present recovery procedure are directly related to the empirical equations adopted for the correction factors. The proposed Eqs. (4) and (6) for n_a and n_v and for λ_a and λ_v, respectively, were chosen taking into account accuracy (highest possible correlation coefficient), simplicity (smallest possible number of parameters) as well as applicability to all categories (bins) of seismic motions considered herein. The highest accuracy and applicability to all bin cases was achieved using Chebyshev polynomials of order 3-8. Nevertheless, the polynomial expressions are not simple and require a large number of parameters.

Finally, the coefficients of variation COV (defined as the ratio of the standard deviation to the mean) for the correction factors λ_a and λ_v are shown in Figs. 5 and 6, respectively. These coefficients shown in Figs. 5 and 6 correspond to the far- and near-field cases of Figs.1-4. Similar figures can be constructed for the rest of far- and near-field motions but are not shown herein due

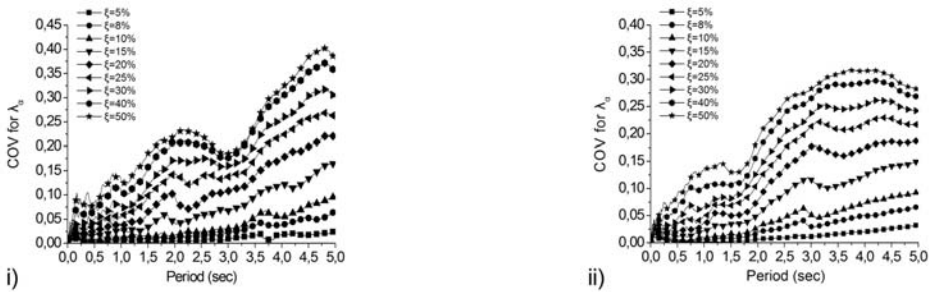

Fig. 5 Coefficients of variation for λ_a for (i) far-field, $6.7 \leq M_w \leq 7.3$, $10 \leq R \leq 40$ km, site class C and (ii) near-field, $M_w \leq 6.7$ motions

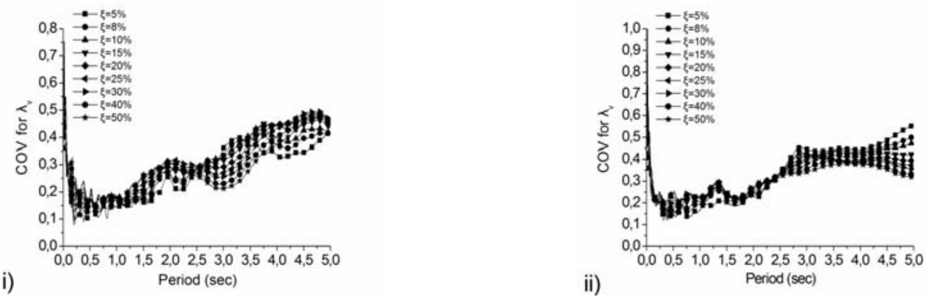

Fig. 6 Coefficients of variation for λ_v for (i) far-field, $6.7 \leq M_w \leq 7.3$, $10 \leq R \leq 40$ km, site class C and (ii) near-field, $M_w \leq 6.7$ motions

to space limitations. From Figs. 5 and 6 the level of the dispersion of the correction factors can be found. It can be said that the correction factors coefficients of variation show differences in distribution that depend on earthquake magnitude, site class and site-to-source distance. In general, as the damping ratio and period increase, COV increases. However, it should be noted that the COV's can neither be used to construct confidence intervals for the mean values nor to validate the empirical equations.

5. Conclusions

On the basis of the preceding developments, the following conclusions can be stated:

(1) In cases where high damping is present, the absolute acceleration and the relative velocity spectra instead of the pseudo-acceleration and the pseudo-velocity spectra should be used.

(2) Spectral absolute acceleration and spectral relative velocity can be recovered from their pseudo- spectral counterparts. This is performed with the aid of correction factors that come out to be functions of period and damping ratio.

(3) Empirical equations of those factors are provided for far-field and near-field seismic motions and various combinations of earthquake magnitude, site class and site-to-source

distance. Using these correction factors the spectral pseudo-acceleration and spectral pseudo-velocity can be easily and accurately enough transformed into spectral absolute acceleration and spectral relative velocity and, thus, the construction of absolute acceleration and relative velocity spectra can be avoided.

References

ATC-40 (1996), *Seismic evaluation and retrofit of concrete buildings*, Applied Technology Council: Redwood City, California.

Bommer, J.J. and Mendis, R. (2005), "Scaling of spectral displacements ordinates with damping ratios", *Earthq. Eng. Struct. D.*, **34**(2), 145-165.

Cameron, W.I. and Green, R.U. (2007), ''Damping correction factors for horizontal ground-motion response spectra'', *B. Seismol. Soc. Am.*, **97**, 934-960.

Cardone, D., Dolce, M. and Rivelli, M. (2009), ''Evaluation of reduction factors for high-damping design response spectra'', *B. Earthq. Eng.*, **7**(1), 273-291.

Eurocode 8 (2004), *Design of structures for earthquake resistance*, Part 1: General rules – Seismic actions and general requirements for structures, European pre-norm ENV 1998-1, CEN: Brussels.

Hatzigeorgiou, G.D. (2010), "Damping modification factors for SDOF systems subjected to near-fault, far-fault and artificial earthquakes", *Earthq. Eng. Struct. D.*, **39**(11), 1239-1258.

Lin, Y.Y. and Chang, K.C. (2003), ''A study on damping reduction factor for buildings under earthquake ground motion'', *J. Struct. Eng.-ASCE*, **129**(2), 206-214.

Lin, Y.Y. and Chang, K.C. (2004), "Effects of site classes on damping reduction factors", *J. Struct. Eng.-ASCE*, **130**(11), 1667-1675.

Lin, Y.Y., Miranda, E. and Chang, K.C. (2005), "Evaluation of damping reduction factors for estimating elastic response of structures with high damping", *Earthq. Eng. Struct. D.*, **34**(11), 1427-1443.

Mavroeides, G.P., Dong, G. and Papageorgiou, A.S. (2004), "Near-fault ground motions, and the response of elastic and inelastic single-degree-of-freedom (SDOF) system", *Earthq. Eng. Struct. D.*, **33**(9), 1023-1049.

Naeim, F. and Kelly, J.M. (1999), *Design of seismic isolated structures*, Wiley: Chichester, UK.

NEHRP (2000), *Recommended provisions for seismic regulations for new buildings and other structures*, Federal Emergency Management Agency (FEMA): Washington, DC.

Newmark, N.M. and Hall, W.J. (1982), *Earthquake spectra and design*, EERI Monograph Series. Earthquake Engineering Research Institute: Oakland, California.

Papagiannopoulos, G.A. and Beskos, D.E. (2010), "Towards a seismic design method for plane steel frames by using equivalent modal damping ratios", *Soil Dyn. Earthq. Eng.*, **30**(10), 1106-1118.

Papagiannopoulos, G.A. and Beskos, D.E. (2011), "Modal strength reduction factors for seismic design of plane steel frames", *Earthq. Struct.*, **2**, 65-88.

Pekcan, G., Mander, J.B. and Chen, S.S. (1999), "Fundamental considerations for the design of non-linear viscous dampers", *Earthq. Eng. Struct. D.*, **29**(7), 1405-1425.

Priestley, M.J.N., Calvi, G.M. and Kowalsky, M.J. (2007), *Displacement based seismic design of structures*, IUSS Press: Pavia, Italy.

Ramirez, O.M., Constantinou, M.C., Whittaker, A.S., Kircher, C.A. and Chrysostomou, C.Z. (2002), "Elastic and inelastic seismic response of buildings with damping systems", *Earthq. Spectra*, **18**, 531-547.

Rupakhety, R., Sigurdsson, S., Papageorgiou, A.S. and Sigbjornsson, R. (2011), "Quantification of ground-motion parameters and response spectra in the near-fault region", *B. Seismol. Soc. Am.*, **9**(4), 893-930.

Sadek, F., Mohraz, B. and Riley, M.A. (2000), "Linear procedures for structures with velocity-dependent dampers", *J. Struct. Eng.-ASCE*, **126**(8), 887-895.

Shibata, A. and Sozen, M.A. (1976), "Substitute-structure method for seismic design in R/C", *J. Struct. Div.-ASCE*, **102**, 1-18.

Song, J., Chu, Y.L., Liang, Z. and Lee, G.C. (2007), "Estimation of peak relative velocity and peak absolute acceleration of linear SDOF systems", *Earthq. Eng. Eng. Vib*., **6**(1), 1-10.

Soong, T.T. and Constantinou, M.C. (1994), *Passive and active structural vibration control in civil engineering*, Springer Verlag: New York.

Stafford, P.J., Mendis, R. and Bommer, J.J. (2008), "The dependence of spectral damping ratios on duration and number of cycles", *J. Struct. Eng.-ASCE*, **134**, 1364-1373.

Table Curve 3D (2002), *Version 4*, SYSTAT Software Inc.

Weitzmann, R., Ohsaki, M. and Nakashima, M. (2006), "Simplified methods for design of base-isolated structures in the long-period high-damping range", *Earthq. Eng. Struct. D*., **35**(4), 497-515.

SA